WATER FRACTIONS IN EXTRASOLAR PLANETESIMALS

M. Jura[a] & S. Xu(许偲艺)[a]

ABSTRACT

With the goal of using externally-polluted white dwarfs to investigate the water fractions of extrasolar planetesimals, we assemble from the literature a sample that we estimate to be more than 60% complete of DB white dwarfs warmer than 13,000 K, more luminous than 3×10^{-3} $L_{\odot}$ and within 80 pc of the Sun. When considering all the stars together, we find the summed mass accretion rate of heavy atoms exceeds that of hydrogen by over a factor of 1000. If so, this sub-population of extrasolar asteroids treated as an ensemble has little water and is at least a factor of 20 drier than CI chondrites, the most primitive meteorites. In contrast, while an apparent "excess" of oxygen in a single DB can be interpreted as evidence that the accreted material originated in a water-rich parent body, we show that at least in some cases, there can be sufficient uncertainties in the time history of the accretion rate that such an argument may be ambiguous. Regardless of the difficulty associated with interpreting the results from an individual object, our analysis of the population of polluted DBs provides indirect observational support for the theoretical view that a snow line is important in disks where rocky planetesimals form.

Subject headings: planetary systems – stars, white dwarf

1. INTRODUCTION

Evidence is now strong that most externally-polluted white dwarfs derive their heavy atoms[1] by accretion from disrupted planetesimals (Jura 2003; Gaensicke et al. 2006; Jura 2008; Farihi et al. 2010; Zuckerman et al. 2010). Observational progress is rapid; both detailed studies of individual objects (Klein et al. 2010, 2011; Dufour et al. 2010; Farihi et al. 2011a,b; Vennes et al. 2010; Melis et al. 2011; Zuckerman et al. 2011) and broader surveys (Koester et al. 2011; Kawka et al. 2011; Zuckerman et al. 2010) are now being performed. Here, we combine recent studies of white dwarfs to assess the water fraction – either in pure form or in hydrated minerals (Rivkin et al. 2002) – within an ensemble of extrasolar minor planets.

[a]Department of Physics and Astronomy, University of California, Los Angeles CA 90095-1562; jura, sxu@astro.ucla.edu

[1]We use "heavy atoms" to mean all elements with atomic number greater than two. We do not follow astronomical convention and use "metals" for this matter because of this word's different meaning in the context of the physics of planets.

Oxygen is so cosmically abundant that H_2O is predicted to be a major constituent in solid planets that form in regions where the temperature in the planet-forming disk is sufficiently low that ice is stable. Water is widespread in the outer solar system (Jewitt et al. 2007; Encrenaz 2008), and can be more than 50% of the mass of Kuiper Belt Objects and comets. Ceres, the largest asteroid, is probably ∼25% water (McCord & Sotin 2005; Thomas et al. 2005) and CI chondrites are nearly 20% water (Wasson & Kallemeyn 1988). In contrast, much of the inner solar system is dry. For example, the refractory-rich CV chondrites are only about 2% water (Wasson & Kallemeyn 1988). Although the amount of internal water is not well known, the water fraction of bulk Earth is between 0.06% and 2% (van Thienen et al. 2007). The usual theoretical explanation for the large radial variation in water content in the solar system is that there is a snow line in the planet-forming disk and that ice forms and condenses into planetesimals only in the cold, outer regions (Encrenaz 2008). Water may be common in some extrasolar planets (Fortney et al. 2007; Seager et al. 2007; Sotin et al. 2007; Valencia et al. 2007), but actual evidence of ice-rich extrasolar planets is sparse and uncertain (Charbonneau et al. 2009; Gould et al. 2010; Tinney et al. 2011).

Because most internal water can survive within an asteroid with a radius greater than 60 km during a 3 $M_\odot$ star's pre-white-dwarf Asymptotic Giant Branch (AGB) evolution (Jura & Xu 2010), measurements of oxygen in an externally-polluted white dwarf's atmosphere[2] can serve as a tool to assess the amount of water in an accreted parent body. Klein et al. (2010) showed that the oxygen accreted by GD 40 could have been carried in oxides such as MgO and SiO_2 and that water is less than 10% by mass of the photospheric pollution. Similarly, in HS 2253+8023 less than 10% of the accreted mass is water (Klein et al. 2011). However, because of the inherent uncertainties in abundance determinations, there is little prospect of using this technique to reduce much below ∼10% by mass the bound on the amount of water carried in the parent bodies.

Water-rich parent bodies might be identified if there is an excess of oxygen (Jura & Xu 2010). Farihi et al. (2011a) proposed that GD 61 has accreted a water-rich asteroid, but, as discussed in Section 3 below, we argue that the evidence in support of this suggestion is inconclusive because their argument is somewhat sensitive to the unknown time history of the accretion rate.

Another pathway to study the water content in extrasolar asteroids is to measure the amount of hydrogen that results from planetesimal accretion onto DB white dwarfs[3] because this light gas never gravitationally settles (Koester 2009). At least 1/3 of DBs warmer than 14,000 K are externally-polluted by heavy atoms derived from ancient planetesimals (Zuckerman et al. 2010). These same stars also acquire whatever hydrogen that was bound into water in the parent body.

[2]Gaensicke et al. (2010) reported dredged-up oxygen in two massive, cool white dwarfs, but there is no known way that the systems we discuss here have internally-polluted atmospheres.

[3]DBs are white dwarfs where the helium lines dominate the spectrum. Related objects are the DBAs where hydrogen also is detected and the DZs which are thought to have helium-dominated atmospheres but are too cool for helium lines to appear in the spectrum.

By assessing the relative amounts of hydrogen and heavy-atoms in the stellar photospheres, we can constrain the amount of water in the accreted planetesimals. For example, Zuckerman et al. (2010) showed that the upper limit to the hydrogen abundance in G241-6 indicates that little water has been accreted.

Because hydrogen accumulates over the entire cooling age of the star and because the white dwarf may have substantial primordial hydrogen (Bergeron et al. 2011), we cannot attribute the observed hydrogen to any particular accretion event. Instead, we consider a well-defined ensemble of white dwarfs and sum the individual hydrogen accumulation rates to compare with the summed heavy atom accretion rates. While particular white dwarfs such as GD 362 have acquired so much hydrogen that they may have accreted ice-rich matter (Jura et al. 2009), here we consider the warm DBs in aggregate. By considering the ensemble as a whole, this procedure can probe much smaller water fractions than allowed by assessing the amount of hydrogen in individual objects. Below, we show that water is less than 1% of the aggregate mass in our sample of extrasolar asteroids, an order of magnitude improvement over what can be achieved by examining each star on a case-by-case basis.

In Section 2, we describe a volume-limited sample of DBs and compare the summed accretion rates of both heavy atoms and hydrogen. In aggregate, the accreted material is dry. In Section 3, we describe models for a quasi-steady state accretion and argue that the evidence that GD 61 is accreting ice-rich material is inconclusive. In Section 4 we discuss some further implications of our analysis, and in Section 5 we present our conclusions.

2. AGGREGATE ACCRETION RATES

2.1. The Sample of Stars

In order to assess the relative amounts of accreted hydrogen and heavy elements, we assemble a volume-limited sample of DBs that is as bias-free as possible. We cannot use the available survey of white dwarfs within 20 pc of the Sun that is nearly complete because it contains only one DB (Holberg et al. 2008). As a compromise between having enough stars to perform an analysis yet not being too incomplete, we adopt the outer boundary of our sample at 80 pc. Because it is difficult to distinguish helium in atmospheres cooler than 13,000 K and such cool DBs are difficult to characterize; we only consider stars warmer than this temperature.

Using available literature, we list in Table 1 57 DBs with luminosities greater than 3×10^{-3} $L_{\odot}$ or $M_{Bol} = 11$ mag, along with their distances, temperatures, galactic latitudes, masses, and accretion rates. According to Bergeron et al. (2011), the space density of such DBs is 5.15×10^{-5} stars pc^{-3}, and we might expect to identify 110 appropriate objects within 80 pc. We now assess the incompleteness of our sample in more detail.

If the stars are distributed isotropically in the sky, we would expect 50% to lie at $|b| \leq 30°$.

However, we only identify 17 stars in this zone. The incompleteness of Table 1 is at least partly because some stars near the Galactic Plane are missed. As demonstrated by Lepine et al. (2011) and as illustrated by the recent discovery of a DAZ at a distance of 55 pc with b = -8° and T_{eff} = 20,900 K (Vennes et al. 2010), there are nearby warm white dwarfs yet to be found in this region.

In actuality, we expect fewer than half the stars lie at $|b| > 30°$ because the space density of stars decreases away from the Galactic Plane with a scale height, h, which depends upon the mass of the main-seqeunce progenitor. Assume that

$$n \; = \; n_0 \; e^{-|r \, \sin b|/h} \tag{1}$$

where n_0 is the local density in the mid-Plane. If so, then the number of stars in a spherical volume of radius D centered on the Sun assumed to lie in the midplane of the Galactic Plane, $N(D)$, can be found from a Taylor series expansion as:

$$N(D) \approx \frac{4\pi \, n_0}{3} \, D^3 \left(1 \, - \frac{3}{8} \, \frac{D}{h} \, + \, \frac{1}{10} \frac{D^2}{h^2} \, - \, ... \right) \tag{2}$$

With D = 80 pc and h no larger than 150 pc (Gilmore & Zeilik 2000), we expect to find no more than 91 DBs. Because we identify 57 stars in Table 1, our sample is at least 60% complete.

Most of the stars in Table 1 are listed in Bergeron et al. (2011) and Voss et al. (2007). When a star is considered in both samples, to be as consistent as possible, we adopt the stellar parameters in Bergeron et al. (2011). For a few stars, only very limited data are available.

One of the most important DBs for our purposes is HS 2253+8023 because it has a large amount of external pollution. The star's gravity is not well constrained in the detailed study of Klein et al. (2011); we adopt their most probable value. The distance to this star is derived from its radius, effective temperature and J-band 2MASS magnitude. We adopt a similar approach to determine distances to the other stars whose distances are not provided by Bergeron et al. (2011).

The average mass of the DBs in Table 1 is 0.67 $M_\odot$. Using the initial mass final mass relation of Williams et al. (2009), this implies a typical main-sequence progenitor mass of 2.5 $M_\odot$.

2.2. Upper Bounds to the Hydrogen Accretion Rates

We now consider a DB's hydrogen budget. For the i'th star, we compute the upper bound to the hydrogen accretion rate averaged over the entire cooling age of the star, $\overline{\dot{M}_i(H)}$, simply as the total mass of accumulated hydrogen, $M_i(H)$, divided by the white dwarf's cooling age, $t_{cool,i}$:

$$\overline{\dot{M}_i(H)} \; = \; \frac{M_i(H)}{t_{cool,i}} \tag{3}$$

As explained in Jura (2011), we expect the loss of accreted hydrogen by the action of a stellar wind to be negligible. To determine $M_i(H)$, we have used reported values of [H]/[He] and models for

the mass of the star's convective zone as a function of stellar gravity and effective temperature. Because Koester (2009) only presented results for one value of white dwarf gravity and hydrogen composition, D. Koester kindly provided a grid of models for DB stars with a sufficient range of temperature, mass and [H]/[He] to enable us to interpolate for the mass of the convective zone for each star individually in Table 1. The estimates of $M_i(H)$ are strongly sensitive to the star's total mass. For example, for DBs with an effective temperature of 13,000 K, the mass of the convective zone is nearly a factor of 200 smaller in a star of 1.1 $M_\odot$ compared to a star of 0.6 $M_\odot$ (Dufour et al. 2010). In most cases, we take [H]/[He] from the optical study of Bergeron et al. (2011), but for a few stars hotter than 20,000 K, we use upper bounds from published ultraviolet observations which are appreciably more sensitive to the hydrogen abundance. All our estimates for $\overline{\dot{M}_i(H)}$ are upper bounds because the white dwarf could possess primordial hydrogen (Bergeron et al. 2011).

As shown in Figure 1, for the seven stars in Table 1 for which both Bergeron et al. (2011) and Voss et al. (2007) derived masses spectroscopically, instead of just adopting an assumed mean, the values of $\overline{\dot{M}_i(H)}$ are systematically lower from our use of the Bergeron et al. (2011) study compared to those in Voss et al. (2007) by an average factor of 4. This substantial discrepancy is the result of four factors all operating in the same direction. First, Bergeron et al. (2011) typically found larger stellar masses. The typical 15% increase in derived mass means that the mass of the convective zone is smaller by approximately a factor of 2. Second, stars with a larger mass take a longer time to cool to the observed effective temperature; this effect might contribute a factor of 1.2 to the estimate of $\overline{\dot{M}_i(H)}$. Third, because the star's gravity is estimated to be higher in the analysis of Bergeron et al. (2011), the ratio of the hydrogen to helium may be found to be as much as a factor of 2 lower than derived by Voss et al. (2007). Finally, there is a different theoretical treatment of convection such that the values of the mass of the convective zone are typically a factor of 1.5 lower in the models of Koester (2009) compared to those used by Voss et al. (2007). The spectroscopically-derived masses derived by Bergeron et al. (2011) usually agree very well with those derived from trigonometric parallaxes, and therefore it seems likely that the values of $\overline{\dot{M}_i(H)}$ derived from their analysis are realistic. It must be recognized, however, that there are uncertainties.

A few stars in Table 1 have remarkably low upper limits to $\overline{\dot{M}_i(H)}$. These stars can be used to place a bound on the space density of interstellar comets (Jura 2011).

2.3. Heavy Atom Accretion Rates

We wish to compare the hydrogen and heavy atom accretion rates. For the i'th star and the j'th element, the time-averaged mass accretion rate from the disk onto the star, $\overline{\dot{M}_i(Z_j)}$, we take

$$\overline{\dot{M}_i(Z_j)} \; = \; \frac{M_i(Z_j)}{t_i(Z_j)} \tag{4}$$

where $M_i(Z_j)$ is the inferred mass of element Z_j in the star's mixing zone where the gravitational settling time is $t_i(Z_j)$. Using Z_{tot} to denote the mass of all the heavy elements, we define for each star the time-averaged total heavy element accretion rate, $\overline{\dot{M}_i(Z_{tot})}$, as:

$$\overline{\dot{M}_i(Z_{tot})} \; = \; \sum_j \overline{\dot{M}_i(Z_j)} \tag{5}$$

In many cases, only calcium is measured because this element is the most easily to detect in optical spectra; the total heavy element accretion rate is extrapolated as described by Zuckerman et al. (2010). The values of $\overline{\dot{M}_i(Z_{tot})}$ are relatively insensitive to the white dwarf mass because, as illustrated in Klein et al. (2010), the settling time scales approximately with the mass of the convective zone.

Three sources of hydrogen in DBs have been proposed: interstellar (Voss et al. 2007), circumstellar (Jura & Xu 2010) and primordial (Bergeron et al. 2011). Because the heavy elements settle while the hydrogen does not, the absence of a correlation in Figure 2 is not a decisive test of any particular model for the source of the DBs' hydrogen.

2.4. Summed Accretion Rates

Although there are nearby DBs that are missed, we assume that in identifying the stars, there is no bias related to their external-pollution. If so, then we can treat the set of stars as a well defined ensemble and therefore compare the average hydrogen and heavy atom accretion with each other in a meaningful manner. We define $\dot{M}_{Sum}(H)$ as:

$$\dot{M}_{Sum}(H) \; = \; \sum_i \overline{\dot{M}_i(H)} \tag{6}$$

For comparison, the summed heavy atom accretion rate, $\dot{M}_{Sum}(Z_{tot})$, is:

$$\dot{M}_{Sum}(Z_{tot}) \; = \; \sum_i \; \overline{\dot{M}_i(Z_{tot})} \tag{7}$$

With estimates in Table 1 of $\overline{\dot{M}_i(Z_{tot})}$ for 2/3 of the stars, and ignoring any contribution from the remaining 1/3 of the stars, $\dot{M}_{Sum}(Z_{tot})$ is 1.6×10^{10} g s^{-1}. Nearly all stars in Table 1 have been examined for hydrogen, and $\dot{M}_{Sum}(H)$ is $\leq 1.4 \times 10^{7}$ g s^{-1}, approximately a factor of 1000 smaller than the rate for heavy atoms. Because some currently-unknown fraction of this hydrogen is derived from the interstellar medium or is primordial, we conclude that in the entire ensemble less than 1% of the accreted mass is carried in water. This bound is only strengthened if there is appreciable accretion of heavy atoms in those stars which have not been examined with high spectral sensitivity. Because we examined 57 stars, the upper bound to the average accretion rate for an individual star is 2.5×10^{5} g s^{-1}.

For both heavy elements and hydrogen, the asummed accretion is dominated by a few stars. If we remove the top three accretors in each category, then $\dot{M}_{Sum}(Z_{tot})$ and $\dot{M}_{Sum}(H)$ are $\leq 2.6 \times 10^9$ g s^{-1} and 4.4×10^6 g s^{-1}, respectively. In this analysis, the ratio of the two accretion rates is approximately a factor of 600. Considered as an aggregate and interpreting the data with the best available parameters, we find that extrasolar asteroids accreted onto the warm DB stars are appreciably drier than CI chondrites.

For the four stars in Table 1 for which comprehensive abundance studies have been performed, we show in Figure 3 a plot of the fraction of the total mass of each of the major individual constituents – O, Mg, Si, Ca and Fe – and the upper bound to the fraction of the toal mass that could have been water. In this Figure, we assume the steady state approximation given by Equation (4). It can be seen that there is a relatively small scatter in most of the mass fractions – especially oxygen, consistent with our treatment of the extrasolar asteroids orbiting separate stars as one population. We also see that the upper limit derived from the analysis of the aggregate population is significantly lower than the limit for any individual star. The individual bounds plotted in Figure 3 are derived by using the lower of the two values for the water fraction in the parent body. The first value which is usually the stronger contraint assumes that all the oxygen in excess of that which could be bound into MgO, SiO_2 and Fe_2O_3 was contained in water. The second value assumes all the atmospheric hydrogen was bound into water. As explained in Section 3, the evidence that GD 61 has accreted ice-rich material is ambiguous, and we therefore plot the water fraction as an upper limit rather than as a measured quantity.

We see in Figure 3 that the extrasolar asteroids are in aggregate drier even than CV chondrites – the most refractory-rich of common meteorites (Wasson & Kallemeyn 1988). We also see that commonly the extrasolar asteroids also are more rich in the refractory element Ca than the CV chondrites. We can understand the dryness of extrasolar asteroids as being a result of their having formed interior to the snow line. We do not yet have a good model to explain the relative enhancement of Ca that is measured in these systems.

3. MODELING INDIVIDUAL ACCRETION EVENTS

Having established statistically that ice is low in abundance within our sample of extrasolar asteroids, we now revisit model interpretations of elemental abundances in individual stars. Because different elements settle at different rates, there is not necessarily a simple proportionality between the relative abundances in the atmosphere of the white dwarf and the fractional masses in the parent body. Koester (2009) described three regimes for an accretion event. Initially, after an asteroid is tidally-disrupted into a disk, there is a build-up of heavy elements in the outer convective zone of the star. In this regime, the relative abundances in the stellar atmosphere directly scale as the abundances in the parent body. However, once the elapsed time since the onset of accretion becomes comparable to the gravitational settling time, the system enters a second phase. In this situation, it has been assumed that the gravitational settling rate balances the accretion rate and an exact

steady state is established. Finally, the disk material is completely accreted and the system enters a third phase when the atmospheric pollution decays with the elements with longer settling times lingering in the atmosphere and nominally appearing overabundant. During the first and second phases, the white dwarf possesses a cricumstellar disk. In the third phase, the disk is dissipated. If the disk is dusty, then we can detect an infrared excess. If, however, the disk is largely gaseous (Jura 2008) then it may not be observationally evident.

From the modeling point-of-view, the second phase is the most uncertain because material is both being added and lost from the mixing zone. In the first phase, material is only being added and in the third phase, material is only being lost. We therefore reconsider models for the second phase of an accretion event and reconsider the assumption of an exact steady state. The physics of the accretion from the disk onto the star is not fully understood; it might be variable. Rafikov (2011a) has argued that Poynting-Robertson drag on the disk is important, but clearly this is only part of the story and the accretion rate may vary significantly (Rafikov 2011b; Belyaev & Rafikov 2011) during a disk's evolution. Observations of the time-variation and profiles of emission lines from the circumstellar matter (Gaensicke et al. 2006, 2007, 2008; Melis et al. 2010) raise the possibility that there are significant changes in the accretion rate. We now consider a quasi steady-state where there is a disk, but, nevertheless, the accretion rate varies in time and the system is not in an exact steady state.

Dupuis et al. (1993) computed models for accretion of heavy atoms from the interstellar medium onto DB white dwarfs. Because they invoked both high rates of accretion from clouds and low rates of accretion from the intercloud medium, their calculations explored the observational consequences of time-varying accretion and showed that the photospheric ratio of Mg to Ca could be dramatically enhanced because Mg gravitationally settles more slowly. While recent evidence demonstrates that the heavy atoms in DBs mainly originate from asteroidal parent bodies, their finding that the star's atmospheric abundances are sensitive to the time-history of the entire system remains valid. Our models extend the previous work of Dupuis et al. (1993).

3.1. Quasi-steady Accretion Model

In the outer mixing zone of a white dwarf, the balance between accretion and settling is governed by the expression (Koester 2009):

$$\frac{dM_*(Z_j)}{dt} \;=\; -\frac{M_*(Z_j)}{t_j} \;+\; \dot{M}_{PB}(Z_j) \tag{8}$$

where $\dot{M}_{PB}(Z_j)$ denotes the accretion rate from the circumstellar disk and is a measure of the composition of the tidally-disrupted parent body[4]. Performing an integration on both sides and

[4]For notational convenience, in this Section, we denote the mass in the mixing zone in each star as $M_*(Z_j)$ instead of $M_i(Z_j)$ as in Section 2.

assuming that $M_*(Z_j) = 0$ at $t = 0$, the solution to Equation (8) is:

$$M_*(Z_j) \;=\; e^{-t/t_j} \int_0^t e^{t'/t_j}\, \dot{M}_{PB}(Z_j)\, dt' \tag{9}$$

Inverting the integral in Equation (9) is required to determine the parent body composition. One approach is to Fourier analyze the accretion rate. Because of the large unknowns, for simplicity, we consider just the illustrative special case of a single Fourier term:

$$\dot{M}_{PB}(Z_j) \;=\; \overline{\dot{M}_{PB}(Z_j)}\, \left(1 \,+\, r\, \sin\omega\, t'\right) \tag{10}$$

Here r and ω are free parameters that characterize the amplitude and frequency of the fluctuations in the accretion rate of the j'th element whose time-average value is $\overline{\dot{M}_{PB}(Z_j)}$. In addition to accretion rate variations intrinsic to the disk, there may be multiple disruptions of parent bodies that also may lead to time variations of the accretion rate (Jura 2008). In all cases, we require $r < 1$.

For convenience, define the dimensionless term:

$$B_j \;=\; t_j\, \omega \tag{11}$$

Then:

$$M_*(Z_j) \;=\; \overline{\dot{M}_{PB}(Z_j)}\;\; t_j\;\left(\left[1 \,-\, e^{-t/t_j}\right] \,+\, \left[\frac{r}{1 \,+\, B_j^2}\right]\left[\sin\omega\, t \;-\; B_j \cos\omega\, t \;+\; B_j\, e^{-t/t_j}\right]\right) \tag{12}$$

It is instructive to consider some limiting case solutions to Equation (12). When $t << t_j$, then:

$$M_*(Z_j) \approx \overline{\dot{M}_{PB}(Z_j)} \tag{13}$$

In this circumstance, the element's mass in the stellar atmosphere directly corresponds to the accretion rate; the initial build-up phase discussed by Koester (2009). When $t >> t_j$, then the solution to Equation (12) is:

$$M_*(Z_j) \approx \overline{\dot{M}_{PB}(Z_j)}\;\; t_j\;\left(1 \,+\, \left[\frac{r}{1 \,+\, B_j^2}\right]\left[\sin\omega\, t \;-\; B_j \cos\omega\, t\right]\right) \tag{14}$$

In the exact steady state where the accretion rate is constant and $r = 0$, then the abundance of an element in the parent body are just given by the abundances in the photosphere divided by the settling time and from Equation (14) we recover Equation (4). However, if $r > 0$, the relationship between the photospheric concentration of an element and its relative abundance in the parent body is not the simple proportionality of Equation (4).

By examination of Equation (14), we can see that the quasi steady-state approximation usually agrees with the exact steady state model by better than a factor of 2. That is if $B_j >> 1$, then clearly

$M_*(Z_j)$ is essentially constant and the limit of Equation (4) is reached. In this case, variations in the accretion time are short compared to the settling time and the pollution mass in the mixing zone is constant. If $B_j << 1$, then $M_*(Z_j)$ might vary substantially, but the variations in the accretion rate are so slow that the system's behavior is very similar to the exact steady state. The only situation when there is a significant difference between the quasi-steady state and the exact steady state is when $B_j \approx 1$. In this case, the settling and accretion times are comparable and the interplay between the two factors can be complex, each element behaving differently according to its specific value of B_j.

3.2. Was the Parent Body Accreting onto GD 61 Ice-Rich?

We now use the model of quasi-steady accretion to address the question of whether the parent body accreted onto GD 61 was ice-rich as proposed by Farihi et al. (2011a). We see in Figure 3 that both G241-6 and GD 61 have relatively high fractions of oxygen in their contaminants, and therefore both systems are candidates for the accreted parent body having had a substantial amount of water. However, G241-6 has little photospheric hydrogen, and therefore less than 10% of the mass fraction of the pollution is water (Klein et al. 2011). Because G241-6 does not have a circumstellar dust disk (Xu & Jura 2011), plausibly, it is in a late phase of an accretion event and the oxygen is especially abundant because it lingers longer in the outer settling zone. In contrast, GD 61 has a substantial amount of hydrogen in its photosphere and a circumstellar dust disk (Farihi et al. 2011a). It is likely that there is ongoing accretion from the disk onto the star, and Farihi et al. (2011a) assume that the GD 61 system is in an exact steady state. If so, then by mass there is about 30% more oxygen than can be locked into oxide minerals and this implies that the parent body contained a substantial amount of ice. This oxygen excess is sufficiently small that the analysis is sensitive to whether the system is in an exact steady state or only a quasi steady state.

One difficulty with using the exact steady state model to interpret the data for GD 61 is that iron displays a relatively low abundance. In an exact steady state model, as shown in Figure 3, it is inferred to have an usually low fractional abundance compared to other polluted white dwarfs. One possible way to explain simultaneously both the low iron and the high oxygen fractional abundances is that the system simply is in a late phase where only settling occurs (Jura & Xu 2010; Klein et al. 2011). However, this hypothesis is inconsistent with the presence of a dust disk and therefore the likelihood that accretion is ongoing. Farihi et al. (2011a) suggested that the accretion onto GD 61 is iron-poor because the circumstellar disk is composed of the outer portion of a planetesimal where most of the iron was concentrated into a central core.

GD 61 is deficient in carbon relative to the Sun by about a factor of 1000 (Desharnais et al. 2008; Farihi et al. 2011a). According to Lee et al. (2010), in planet-forming disks, carbon should be treated as a volatile which therefore explains why this element is commonly observed to have a low abundance in extrasolar asteroids (Jura 2006). If, in fact, the parent body accreted onto GD 61 was ice-rich, it would be a puzzle to understand why it was simultaneously carbon-poor.

Here, we suggest that a quasi-steady state model may explain the data without any requirement that the accreted parent body contained ice. Therefore, our input parameters are chosen to find the largest effect of the quasi static model; they are not necessarily physically realistic. Consequently, using Equation (14), we compute a model with $\omega = 0.8 \times 10^{-5}$ yr^{-1} and $r = 0.95$. Because the gravitational settling times typically are $\sim 10^5$ yr (Farihi et al. 2011a), this choice of ω means that the values of B_j are nearly 1. The relative mass fractions of O, Mg, Si and Fe are taken to equal 0.40, 0.18, 0.20 and 0.22; these relative abundances are close to the values for bulk Earth (Allegre et al. 2001) except for iron which is about 50% too low. However, because the error in the photospheric abundance of Fe in GD 61 is 0.2 dex (Farihi et al. 2011a), the true fractional abundance of this element in the parent body is not required to be anomalously low compared to bulk Earth.

We display in Figure 4 the results of our model calculation for the fractional abundances in the photosphere at different times. We see that there is a phase when the model matches the data. It therefore seems that the argument that there must be water in the parent body accreted onto GD 61 is provisional.

4. DISCUSSION

Hydrogen and oxygen are sufficiently cosmically abundant that in a disk where gas condenses into solids at least half of the total mass could be ice. If, however, the temperature is high enough, only relatively refractory materials enter the solid phase and eventually are incorporated into planetesimals. Because the temperature in a disk decreases radially from the central star, it is likely that ice-rich objects form in cold, distant regions. We find that water is less than 1% of the mass of the ensemble of extrasolar asteroids accreted onto DB white dwarfs, and therefore these planetesimals likely formed interior to the snow line, the theoretical boundary between the ice-forming and the ice-free zones.

We have argued that oxygen is not sufficiently enhanced in GD 61's heavy element contamination to demonstrate convincingly that there was water within the parent body. In the future, a polluted white dwarf might be identified where the oxygen is sufficiently more abundant than the other species that the argument for water could be more convincing. In GD 40's photosphere, the number of O atoms is a factor of 2.3 times greater than the sum of the number of Mg, Si and Fe atoms (Klein et al. 2010). In this star, there is no evidence for any ice in the accreted parent body. In GD 61's photosphere, the number of O atoms is a factor of 2.9 times greater than the sum of the number of Si, Mg and Fe atoms (Farihi et al. 2011a). In this star, there may have been water in the parent body, but the case is uncertain. In the Sun, the number of O atoms is 4.9 times greater than the sum of Mg, Si and Fe atoms (Lodders 2003). A planetesimal that formed in a very cold environment could have a correspondingly large fraction of oxygen. If this object is accreted onto a white dwarf, its very high oxygen fraction could be measured and the case would be good for an ice-rich parent body. However, if the white dwarf is a DB, then the settling times are sufficiently

long that unless there was also evidence for ongoing accretion, it might be difficult to exclude the possibility that the enhancement of oxygen is simply the consequence of its lingering longer in the mixing zone.

We could hope to use warm DA white dwarfs to study relative oxygen abundances because the settling times are shorter than a year and the system almost certainly is in a steady state (Koester 2009). Unfortunately, the current situation is murky. GALEX J1931 is an exceptionally heavily polluted DA where all the major element contaminates are measured, and the number of O atoms in the photosphere is somewhere between 1.0 and 1.8 times the sum of the Mg, Si and Fe atoms (Vennes et al. 2010, 2011a; Melis et al. 2011). The two groups do not agree very well in their determination of the iron abundance, perhaps because Vennes et al. (2010) only used one weak Fe line while Melis et al. (2011) used several iron lines. More importantly for our purposes here, correcting for settling and consequent stratification through the atmosphere, the number of O atoms compared to the sum of Mg, Si and Fe atoms is either $\sim$11 (Vennes et al. 2010) or $\sim$1 (Melis et al. 2011). In the first case, likely the parent body was ice-rich; in the second case likely it was ice-poor. Because we have found that ice-rich parent bodies are not ubiquitous; observations of additional DA stars may help resolve this disagreement. The analysis of DB stars does not suffer this particular ambiguity.

In our toy model for external pollution, we have assumed that the ultimately-accreted hydrogen is chemically bound to oxygen in the form of water. Another possibility is that this hydrogen could be chemically bound to carbon in the form of hydrocarbons. However, carbon is highly volatile in planet-forming environments (Lee et al. 2010) and deficient in those relatively few polluted white dwarfs where it has been studied (Jura 2006; Farihi et al. 2009). Therefore, H_2O is the most likely carrier of hydrogen in extrasolar minor planets. This water could be contained in hydrated silicates such as serpentine rather than pure ice (Rivkin et al. 2002; Wasson 2008).

A large source of uncertainty in our estimates to the upper bounds to the hydrogen accretion rates is the accuracy of the adopted white dwarf masses. This difficulty should be eased with the *Gaia* mission which will determine trigonometric parallaxes of all nearby white dwarfs, greatly extending the work of the *Hipparcos* satellite (Vauclair et al. 1997).

5. CONCLUSIONS

We argue that the aggregated external pollution from parent bodies accreted onto DB white dwarfs is less than 1% by mass composed of water. Consequently, on average, the asteroids that orbited main-sequence stars of typically 2.5 $M_\odot$ are drier than CI chondrites by at least a factor of 20. In contrast, we show that for an individual star such as GD 61, having a large fraction of oxygen in the polluted material does not necessarily imply accretion from a water-rich parent body. Despite the ambiguity associated with studying any single white dwarf, our analysis of the aggregate population of polluted DBs provides indirect observational support that snow lines in

planet-forming disks are common.

We thank D. Koester for providing a grid of models for the masses of white dwarfs and for useful email exchanges. We thank the anonymous referee for thoughtful and constructive comments. This work has been partly supported by the National Science Foundation.

REFERENCES

Allegre, C., Manhes, C., & Lewin, E. 2001, Earth Planet Sci. Lett., 185, 49

Belyaev, M., & Rafikov, R. 2011, ApJ, in press

Bergeron, P. et al. 2011, ApJ, 737, 28

Castanheira, B. G., Kepler, S. O., Handler, G., & Koester, D. 2006, A&A, 450, 331

Charbonneau, D. et al. 2009, Nature, 462, 891

Desharnais, S., Wesemael, F., Chayer, P., Kruk, J. W., & Saffer, R. A. 2008, ApJ, 672, 540

Dufour, P., Kilic, M., Fontaine, G., Bergeron, P., Lachapelle, F., Kleinmann, S. J., & Leggett, S. K. 2010, ApJ, 719, 803

Dupuis, J., Fontaine, G., Pelletier, C., & Wesemael, F. 1993, ApJS, 84, 73

Encrenaz, T. 2008, ARA&A, 46, 57

Farihi, J., Jura, M., & Zuckerman, B. 2009, ApJ, 694, 805

Farihi, J., Barstow, M. A., Redfield, S., Dufour, P., & Hambly, N. C. 2010, MNRAS, 404, 2123

Farihi, J., Brinkworth, C. S., Gaensicke, B. T., Marsh, T. R., Girven, J., Hoard, D. W., Klein, B., & Koester, D. 2011a, ApJ, 728, L8

Farihi, J., Dufour, P., Napiwotzki, R., & Koester, D. 2011b, MNRAS, 413, 2559

Fortney, J., Marley, M. S., & Barnes, J. W. 2007, ApJ, 659, 1661

Gaensicke, B. T., Marsh, T. R., Southworth, J., & Rebassa-Mansergas, A. 2006, Science, 314, 1908

Gaensicke, B. T., Marsh, T. R., & Southworth, J. 2007, MNRAS, 380, L35

Gaensicke, B. T., Koester, D., Marsh, T. R., Rebassa-Mansergas, A., & Southworth, J. 2008, MNRAS, 391, L103

Gaensicke, B. T., Koester, D., Girven, J, Marsh, T. R., & Steeghs, D. 2010, Science, 327, 188

Gilmore, G., & Zeilik, M. 2000, in Allen's Astrophysical Quantities, ed. A. N. Cox (New York: Springer), 471

Gould, A. et al. 2010, ApJ, 720, 1073

Holberg, J. B., Sion, E. M., Oswalt, T., McCook, G. P., Foran, & S., Subasavage, J. P. 2008, AJ, 135, 1225

Jewitt, D., Chizmadia, L., Grimm, R., & Prialnik D. 2007, in Protostars and Planets V, B. Reipurth, D. Jewitt & K. Keil, eds., (University of Arizona Press: Tucson), 863

Jura, M. 2003, ApJ, 584, L91

Jura, M. 2006, ApJ, 653, 613

Jura, M. 2008, AJ, 135, 1785

Jura, M., Muno, M. P., Farihi, J., & Zuckerman, B. 2009, ApJ, 699, 1473

Jura, M., & Xu, S. 2010, AJ, 140, 1129

Jura, M. 2011, AJ, 141, 155

Kawka, A., Vennes, S., Dinnbier, F., Cibulkova, H., & Nemeth, P. 2011, in Planetary Systems Beyond the Main Sequence, American Institute of Physics Conference 1331, 238

Klein, B., Jura, M., Koester, D., Zuckerman, B., & Melis, C. 2010, ApJ, 709, 650

Klein, B., Jura, M., Koester, D., & Zuckerman, B. 2011, ApJ, in press

Koester, D. 2009, A&A, 498, 517

Koester, D., Girven, J., Gaensicke, B. T., & Dufour, P. 2011, A&A, 530, 114

Lee, J.-E., Bergin, E. A., & Nomura, H. 2010, ApJ, 710, L21

Lepine, S., Bergeron, P., & Lanning, H. H. 2011, AJ, 141, 96

Lodders, K. 2003, ApJ, 591, 1220

McCord, T. B., & Sotin, C. 2005, J. Geophys. Res., 110, 5009

Melis, C., Jura, M., Albert, L., Klein, B. & Zuckerman, B. 2010, ApJ, 722, 1078

Melis, C., Farihi, J, Dubour, P., Zuckerman, B., Burgasser, A. J., Bergeron, P., Bochanski, J., & Simcoe, R. 2011, ApJ, 732, 90

Petitclerc, N., Wesemael, F., Kruk, J. W., Chayer, P., & Billeres, M. 2005, ApJ, 624, 317

Rafikov, R. 2011a, ApJ, 732, L3

Rafikov, R. 2011b, MNRAS, 416, L55

Provencal, J. L., Shipman, H. L., Thejll, P., & Vennes, S. 2000, ApJ, 542, 1041

Rivkin, A. S., Howell, E. S., Vilas, F., & Lebofsky, L. A. 2002, in Asteroids III, W. F. Bottke, A. Cellio, P. Paolicchi, & R. P. Benzel, eds., (Tucson; University of Arizona Press), 235

Seager, S., Kuchner, M., Hier-Majumder, C. A., & Militzer, B. 2007, ApJ, 669, 1279

Sion, E. M., Fritz, M. L., McMullin, J. P., & Lallo, M. D. 1988, AJ, 96, 251

Sotin, C., Grasset, O., & Mocquet, A. 2007, Icarus, 191, 337

Subasavage, J. P., Henry, T. J., Bergeron, P., Dufour, P., & Hambly, C. 2008, AJ, 136, 899

Thomas, P. C., Parker, J. Wm., McFadden, L. A., Fussell, C. T., Stern, S. A., Sykes, M. V., & Young, E. F. 2005, Nature, 437, 224

Tinney, C. G., Butler, R. P., Jones, H. R. A., Wittenmyer, R. A., O'Toole, S., Bailey, J., & Carter, B. D. 2011, ApJ, 727, 103

Valencia, D., Sasselov, D. D., & O'Connell, R. J. 2007, ApJ, 656, 545

Vauclair, G., Schmidt, H., Koester, D., & Allard, N. 1997, A&A, 325, 1055

Vennes, S., Kawka, A., & Nemeth, P. 2010, MNRAS, 404, L40

Vennes, S., Kawka, A., & Nemeth, P. 2011a, MNRAS, 413, 2545

van Thienen, P., Benzerara, K., Breuer, D., Gillmann, C., Labrosse, S., Lognonne, P., & Spohn, T. 2007, Space Sci. Rev., 129, 167

Voss, B., Koester, D., Napiwotzki,R., Christlieb, N., & Reimers, D. 2007, A&A, 470, 1079

Xu, S., & Jura, M., ApJ, in press

Wasson, J. D., & Kallemeyn, G. W. 1988, Phil. Trans. R. Soc. A., 325, 535

Wasson, J. T. 2008, Icarus, 195, 895

Williams, K. A., Bolte, M., & Koester, D. 2009, ApJ, 693, 335

Zuckerman, B., Melis, C., Klein, B., Koester, D., & Jura, M. 2010, ApJ, 722, 725

Zuckerman, B., Koester, D., Dufour, P., Melis, C., Klein, B., & Jura, M. 2011, ApJ, in press

Table 1 – DBs Within 80 pc of the Sun

Star (WD)	Name	d (pc)	b (°)	T_{eff} (K)	M_{wd} ($M_\odot$)	log $\overline{\dot{M}(H)}$ (g s^{-1})	log $\overline{\dot{M}(Z_{tot})}$ (g s^{-1})	Notes
0002+729	GD 408	32	+11	14,410	0.75	≤4.39	7.83	(1), (2)
0017+136	Feige 4	75	-48	18,130	0.65	≤5.24		(1)
0100-068	G270-124	43	-69	19,800	0.64	≤3.63	7.70	(1), (3)
0125-236	G274-39	61	-81	16,610	0.75	≤4.70	7.50	(1), (2)
0138-559	BPM 16571	51	-60	15,800				(4)
0300-013	GD 40	64	-49	15,300	0.67	≤4.51	9.44	(1), (5)
0308-565	BPM 17088	50	-52	23,000	0.63	<0.50	<	(1), (6)
0414-0434	HE	61	-36	13,470	0.67	≤5.14	<	(1), (7)
0418-539	BPM 17731	76	-44	19,050	0.66	<4.70	<	(1), (7)
0435+410	GD 61	52	-04	16,810	0.70	≤5.91	8.81	(1), (8)
0437+138	LP475-242	45	-21	15,120	0.74	≤5.63		(1)
0503+147	KUV	31	-15	15,610	0.64	≤5.20		(1)
0517+771	GD 435	69	+22	13,150	0.67	≤4.80	<5.92	(1), (2)
0615-591	NLTT 16355	37	-27	15,750	0.61	<4.32	<	(1), (7)
0716+404	GD 85	59	+22	17,150	0.64	<4.16	<6.8	(1), (9)
0840+262	Ton 10	49	+35	17,770	0.78	≤5.61		(1)
0845-188	NLTT 20260	75	+15	17,470	0.68	< 3.97	<7.53	(1), (2)
0948+013	PG	77	+40	16,810	0.65	≤4.93	<	(1), (7)
1009+416	KUV	69	+55	16,480	1.00	<4.00		(1)
1011+570	GD 303	48	+49	17,350	0.67	<5.05	8.84	(1), (2)
1046-017	GD 124	70	+48	14,620	0.68	<4.14	<6.20	(1), (2)
1107+265	GD 128	78	+67	15,060	0.65	≤5.31	7.17	(1), (2)
1129+373	PG	74	+70	13,030	0.68	≤4.67	<6.07	(1), (2)
1333+487	GD 325	35	+67	15,320	0.61	<5.35		(1)
1336+123	NLTT 34784	51	+71	15,950	0.60	<4.41	<	(1), (7)
1352+004	PG	69	+59	13,980	0.62	≤5.60	7.37	(1), (2)
1403-010	G64-43	80	+56	15,420	0.65	≤4.48	<6.44	(1), (2)
1411+218	PG	38	+71	14,910	0.62	<5.34	<6.26	(1), (2)
1425+540	G200-40	56	+58	14,490	0.56	≤6.86	7.73	(1), (2)
1444-096	PG	52	+44	17,040	0.75	≤4.11	<	(1), (7)

Table 1 – Continued

Star (WD)	Name	d (pc)	b (°)	T_{eff} (K)	M_{wd} $M_\odot$	log $\overline{\dot{M}(H)}$ (g s^{-1})	log $\overline{\dot{M}(Z_{tot})}$ (g s^{-1})	Notes
1459+821	G256-18	49	+34	15,850	0.65	<5.20	<6.36	(1), (2)
1542+182	GD 190	67	+49	22,630	0.63	<0.58	<	(1), (6)
1557+192	KUV	78	+46	19,570	0.68	≤4.48	<	(1), (7)
1610+239	PG	50	+45	13,360	0.69	<5.13	<6.11	(1), (2)
1644+198	PG	56	+36	15,190	0.66	<5.17	6.76	(1), (2)
1645+325	GD 358	46	+39	24,940	0.57	<1.14		(1), (10)
1703+319	PG	67	+35	14,430	0.88	≤4.37		(1)
1708-871	BPM 921	58	-26	23,980	0.64	<1.31		(1)
1709+230	GD 205	65	+32	19,610	0.65	≤4.87	8.73	(1), (2)
1726-578	BPM 24886	51	-13	14,320	0.71	≤5.05		(1)
1822+410	GD 378	45	+22	16,230	0.60	≤6.20	8.58	(1), (2)
1919-362	SCR J1920-3611	42	-21	27,800	0.59			(11)
1940+374	NLTT 48137	47	+07	16,630	0.64	<5.22	<6.73	(1), (2)
2034-532	BPM 26944	35	-37	17,160	0.90	<3.63		(1)
2129+000	G26-10	49	-35	14,380	0.75	<3.88	<6.01	(1), (2)
2130-047	GD 233	50	-38	18,110	0.66	≤4.07	<7.40	(1), (2)
2144-079	GJ837.1	49	-42	16,340	0.70	<4.00	8.08	(1), (2)
2154-437	BPM 44275	61	-52	16,700	0.60	≤5.68	<	(7)
2222+683	G241-6	65	+10	15,230	0.71	<4.97	9.30	(1), (2)
2224-344	LTT 9031	72	-58	19,000				(12)
2229+139	PG	76	-37	14,940	0.70	≤5.75		(1)
2236+541	KPD	79	-04	15,470	0.78	<4.76		(1)
2253-062	GD 243	63	-55	17,190	0.64	≤5.90	<	(1), (7)
2253+8023	HS	71	+19	14,400	0.84	≤4.43	9.95	(13)
2310+175	PG	64	-39	15,170	0.82	<4.55		(1)
2328+510	GD 410	53	-10	14,460	0.63	<5.30		(1)
2334-4127	HE	80	-69	18,250	0.61	≤4.55	<	(7)

The entries in the column for $\overline{\dot{M}(H)}$ may be blank (no measurement reported in the literature), < (no hydrogen detected, but an upper limit is reported) or ≤ (hydrogen detected, but the rate of accretion is an upper limit because there could be some primordial hydrogen). We enter "<" in the log

$\overline{\dot{M}(Z_{tot})}$ column for those stars examined in the SPY survey that do not display any calcium absorption but no quantitative upper limit is provided (Voss et al. 2007). Notes: (1) Bergeron et al. (2011); (2) Zuckerman et al. (2010); (3) Desharnais et al. (2008); (4) Sion et al. (1988); (5) Klein et al. (2010); (6) Petitclerc et al. (2005); (7) Voss et al. (2007); (8) Farihi et al. (2011a); (9) Dupuis et al. (1993); (10) Provencal et al. (2000); (11) Subasavaget et al. (2008); (12) Castanheira et al. (2006); (13) Klein et al. (2011);

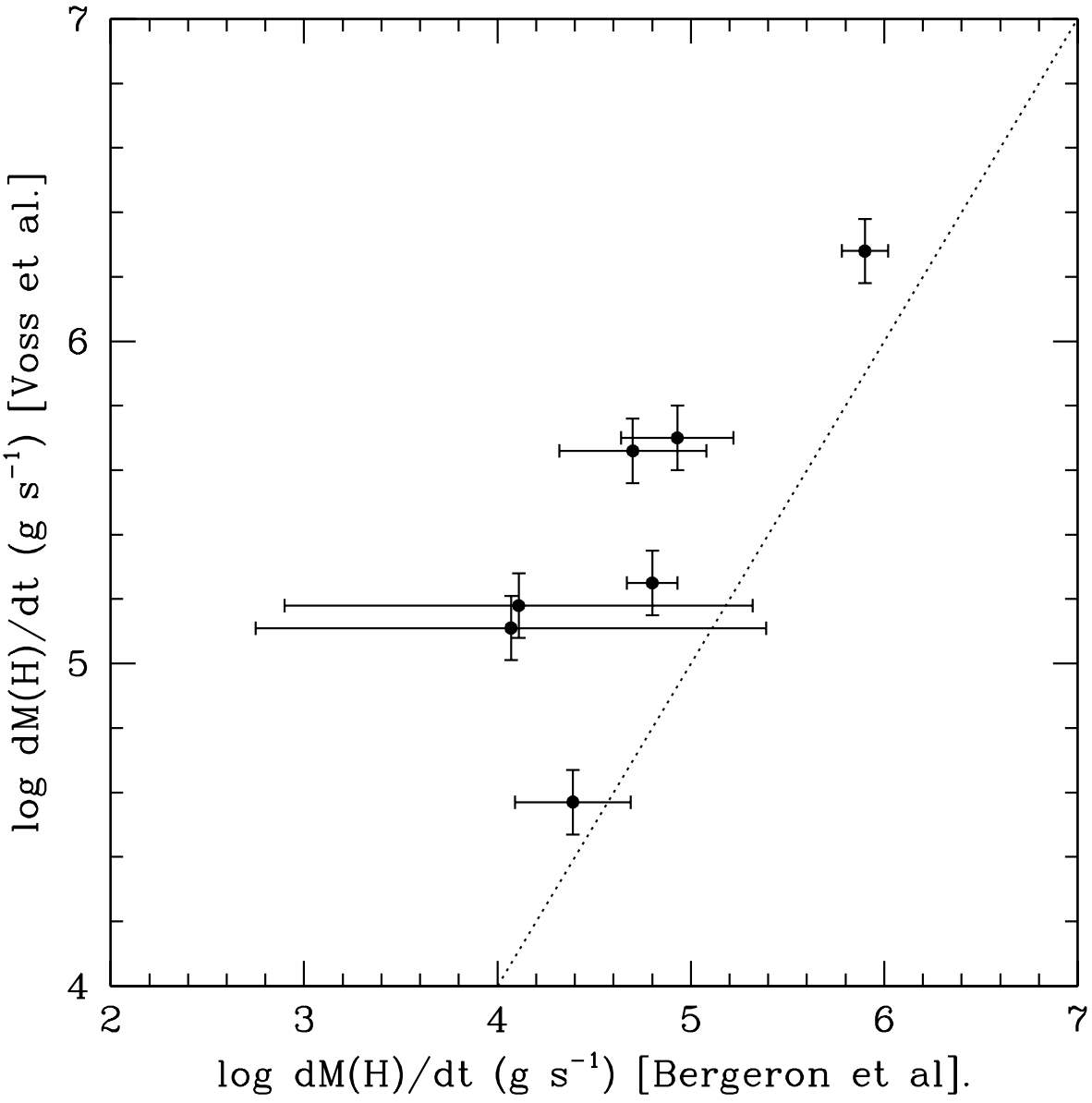

Fig. 1.— Comparison of time-averaged upper bounds to the hydrogen accretion rates, denoted $\dot{M}(H)$ in the text, using the parameters in Voss et al. (2007) and Bergeron et al. (2011) for the seven stars in Table 1 for which both studies derived masses spectroscopically. The dotted line displays the locus of points where the two rates would agree. As discussed in the text, the difference between the two studies is largely the result of Bergeron et al. (2011) deriving higher white dwarf masses. The errors are only those associated with the atmospheric abundance determinations; they do not reflect uncertainties in the stellar mass or effective temperature. While Voss et al. (2007) found that the uncertainties in their derived hydrogen abundances might be as low as 6%, our plotted error bars reflect our assumption that realistically, the errors may be as large as 0.1 dex.

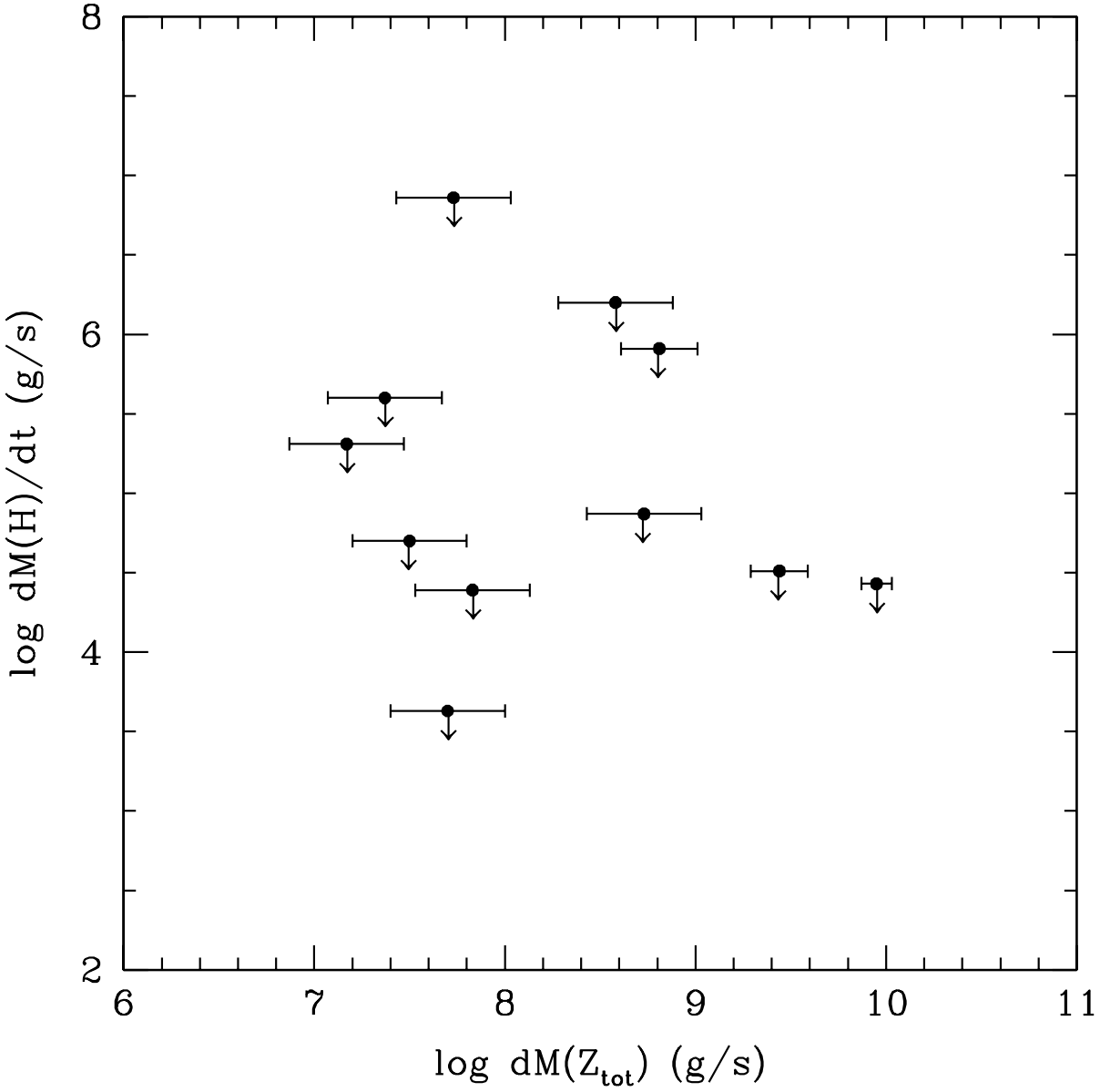

Fig. 2.— Comparison of the upper bound to the time-averaged hydrogen accretion rates, denoted $\overline{\dot{M}(H)}$ in the text, with heavy atom accretion rates, denoted $\overline{\dot{M}(Z_{tot})}$ in the text, for the stars in Table 1 where both quantities are determined. For the stars where only the calcium abundance is reported, we assume an overall uncertainty of a factor of two in the total heavy-atom accretion rate. For the stars with detailed abundance analysis, the plotted error bars are taken from the papers where the data are reported. No correlation between hydrogen accretion and heavy atom accretion is evident.

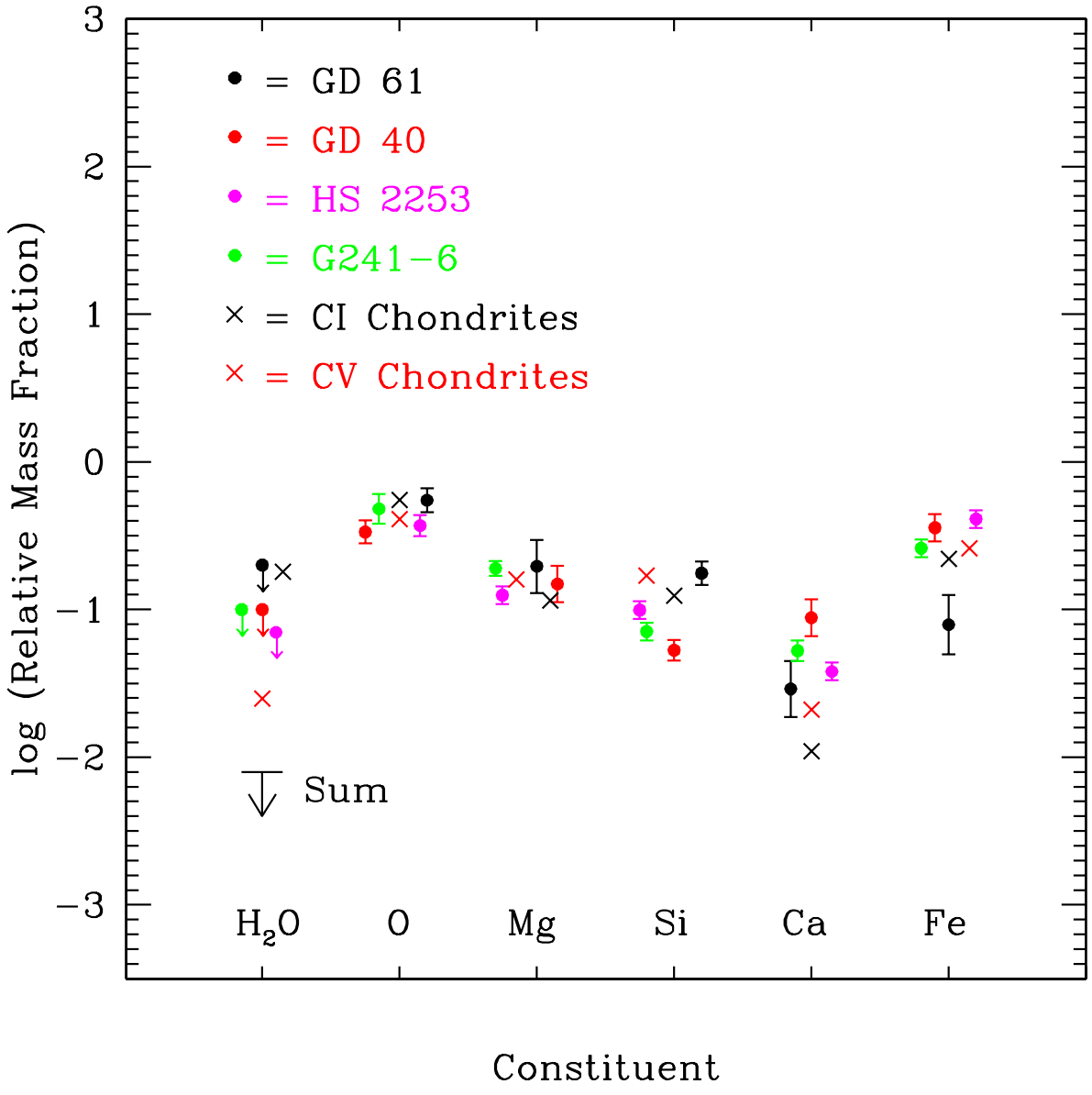

Fig. 3.— The relative fraction of the total mass of the accreted parent body carried by individual constituents for the polluted white dwarfs in Table 1 where all dominant elements – O, Mg, Si, Ca and Fe – have been measured. The upper limit labeled with "Sum" is the bound placed on the fractional aggregate water content of extrasolar asteroids in Section 2. The abundances assigned to the parent bodies accreted onto GD 61 (Farihi et al. 2011a), GD 40 (Klein et al. 2010), G241-6 (Zuckerman et al. 2010) and HS 2253+8023 (Klein et al. 2011) are all corrected from the atmospheric abundances by assuming a steady state and therefore using Equation (4). The water fractions for the white dwarfs are all presented as upper limits; the case of GD 61 is discussed in detail in Section 3.2. The water fractions for solar system CI and CV chondrites are shown for comparison; they are computed by assuming all the hydrogen in the meteorites is carried in water in the form of hydrated minerals.

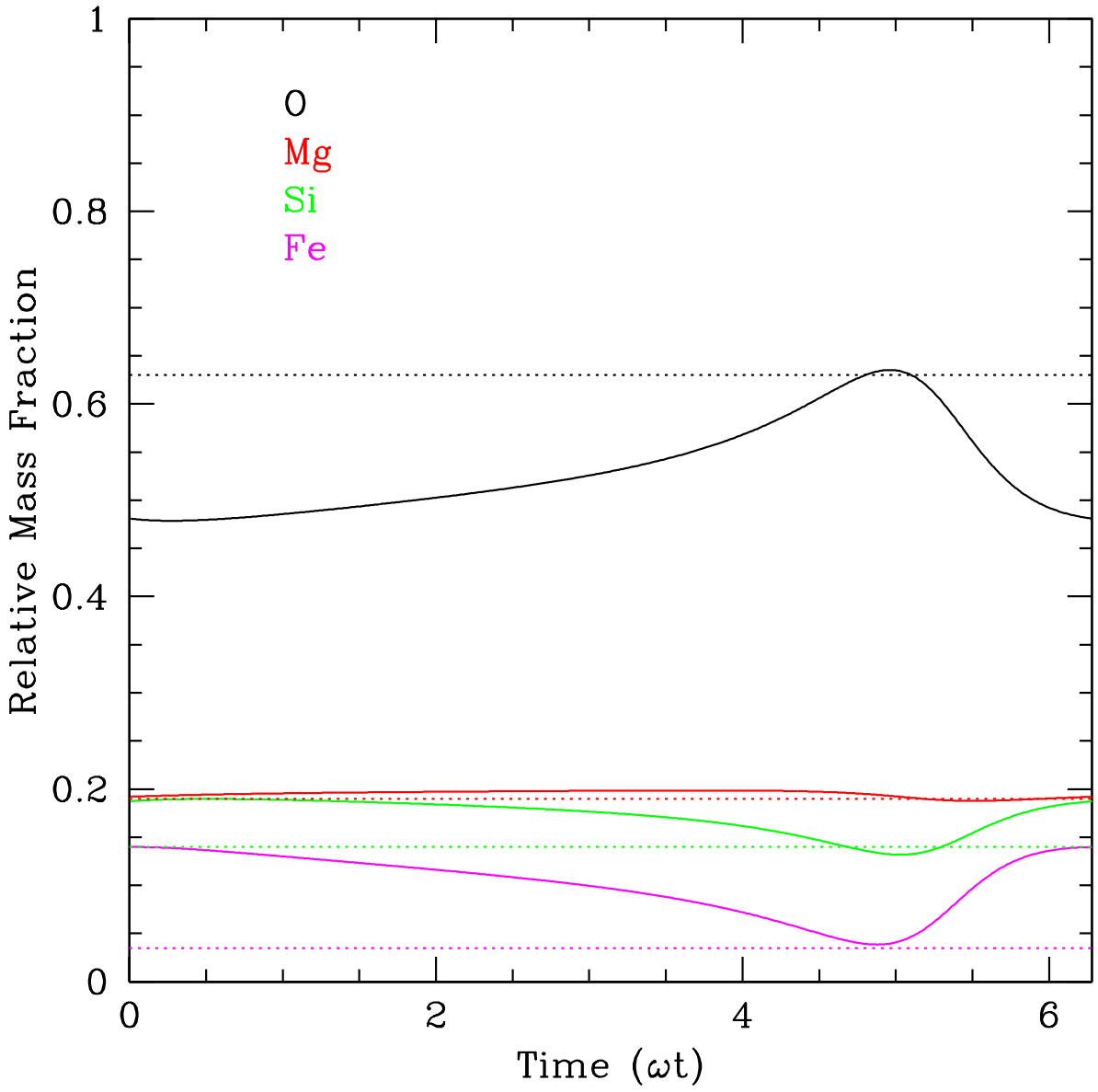

Fig. 4.— Predicted relative mass fractions of individual heavy elements from the accreted parent body within the photosphere of GD 61 in the quasi-steady state model given by Equation (13) with the parameters provided in the text. The dotted horizontal lines display the values measured by Farihi et al. (2011a) and the solid curves the prediction as a function of time scaled to dimensionless units. Even though there is no ice in the model parent body, at $\omega t \approx 4.9$, the data are well matched by the model. The computed fraction of the contamination that is oxygen is always greater than the assumed value in the parent body of 0.4 because oxygen settles relatively slowly compared to the heavier elements.